FAILURE MECHANISMS IN BRITTLE LAMINATES

Akke S.J. Suiker[1] and Norman A. Fleck[2]
[1] Faculty of Aerospace Engineering, Delft University of Technology, Delft, The Netherlands,
[2] Department of Engineering, Cambridge University, Cambridge, UK

ABSTRACT

Steady-state tunneling and plane-strain delamination of an H-shape crack are examined for elastic, isotropic multi layers. Both tunneling and delamination are analysed by employing linear elastic fracture mechanics within a 2D finite element framework. Failure maps are produced to reveal the sensitivity of cracking path to the relative toughness of layer and interface, and to the stiffness mismatch of layers.

1 INTRODUCTION

The fatigue and fracture behaviour of fibre-metal laminates and fibre-reinforced ceramic-matrix composites is of current technological interest because of the increasing number of applications enjoyed by these materials in aerospace engineering, transport industry and general engineering. A typical laminate structure is an alternating stack of aluminium alloy sheets and fibre-reinforced epoxy layers. Laminates reinforced by aramid and glass fibres are commercially known as ARALL and GLARE, respectively, and have been extensively tested over the past 15 years (Vlot and Gunnink, [1]). It has been found experimentally that these laminates are fatigue-resistant since the fibre-epoxy layers arrest the transverse growth of a mode I crack in the metal layer. Instead, the crack tunnels, see Figure 1.

Over the last two decades, the mechanics of crack branching at an interface between two dissimilar materials has been studied for various geometries. An extensive overview of studies on interface delamination can be found in Hutchinson and Suo [2]. The current study considers possible crack propagation paths for alternating layers of two dissimilar but isotropic elastic, brittle solids, designated as materials '1' and '2' in Figure 1. The initiation/nucleation phase of cracking is neglected, and it is assumed that the crack has grown from a large pre-existing flaw in the mid-layer (material 1). The competition is addressed for: (i) tunneling of a mode I crack in the mid-layer with delamination absent (mechanism 1), (ii) tunneling of an H-shape crack with constant delamination length (mechanism 2), and (iii) unstable delamination in all directions (mechanism 3). Failure mechanism maps are constructed to reveal the sensitivity of the operative cracking mechanism to the relative toughness of layer and interface, and to the stiffness mismatch of the layers. The application of the present model is demonstrated in Suiker and Fleck [3,4] through comparisons with experimental data for the residual strength and the fatigue crack growth rate in fibre-metal laminates.

Although tunneling is a 3D phenomenon, the remote stress for steady-state tunneling can be computed from a plane-strain elasticity solution for an H-shape crack: the difference in strain energy upstream and downstream of the tunneling crack front is equated to the delamination work and, for simplicity, the delamination toughness G_{dc} is taken to be independent of the mode-mix (Hutchinson and Suo [2], Beuth, [5], Cox and Marshall [6]). This assumtpion does not induce large errors: in the present study the mode-mix attains a steady-state value at relatively small delamination lengths.

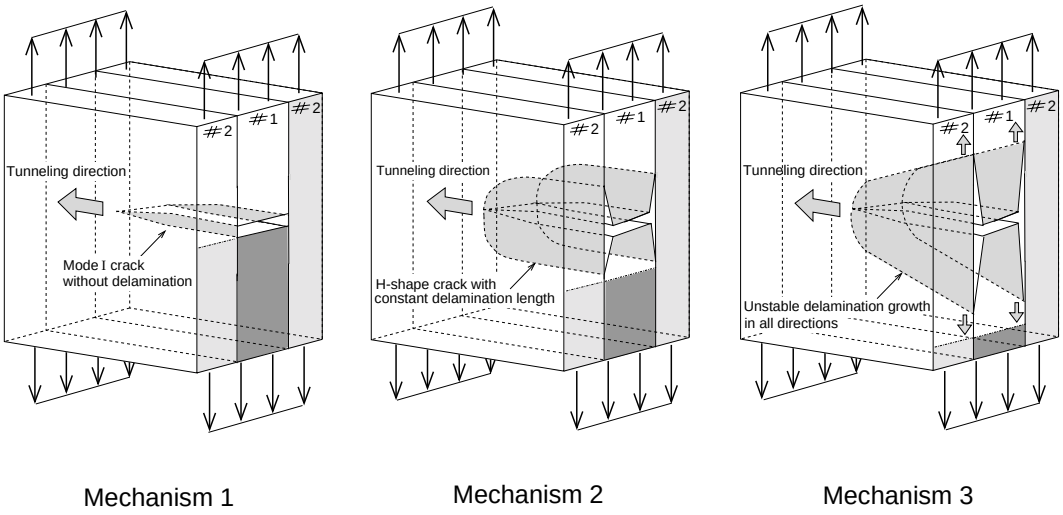

Figure 1: Three possible failure mechanisms for a laminate of two dissimilar, isotropic materials. *Mechanism 1* : Tunneling of a mode I crack without delamination. *Mechanism 2* : Tunneling of an H-shape crack with constant delamination length. *Mechanism 3* : Unstable delamination growth in all directions.

2 STEADY-STATE TUNNELING AND PLANE-STRAIN DELAMINATION

Consider the case of an H-shape crack tunneling within a symmetric stack of 3 layers as shown in Figure 2a; it is assumed that the tunneling crack has nucleated from a flaw within material 1 and is driven by a remote load, characterised by a (uniform) tensile strain ε_{inf}, where the subscript 'inf' denotes 'infinity'. The strain level may either represent static or fatigue loading. The Poisson ratios of the materials are assumed to be equal and representative of many fibre-reinforced laminates, $\nu_1 = \nu_2 = 0.3$. The stiffness mismatch is expressed in terms of the ratio of plane-strain stiffness moduli, $\bar{E}_2/\bar{E}_1$. The H-shape crack comprises a mode I crack of width $2a$ within material 1, and four delaminations each of length l, as depicted in Figure 2a. During steady-state tunneling the tunneling front has a constant shape, and the energy release rate is independent of the tunneling length (and of the geometry of the initial flaw from which the tunneling crack initiated). Then, the energy released per unit tunneling depth can be computed as the difference in elastic strain energy ΔW upstream and downstream of the tunneling front (Hutchinson and Suo [2], Beuth [5], Ho and Suo [7]). This energy drop equals the difference in strain energy for an uncracked plane-strain solid and for a cracked plane-strain solid. For the H-shape crack of Figure 2a the energy drop equals

$$\Delta W = \frac{1}{2}\,\sigma_{inf,1}\,\bar{\delta}\,2a, \tag{1}$$

where $\sigma_{inf,1}(=\bar{E}_1\,\varepsilon_{inf})$ equals the remote tensile stress in material 1 and $\bar{\delta}$ equals the average displacement over the mode I crack faces, according to

$$\bar{\delta} = \frac{1}{2a}\int_{-a}^{a} \delta(x)\,\mathrm{d}x. \tag{2}$$

By dimensional considerations, the average displacement $\bar{\delta}$ may be written in the form

$$\bar{\delta} = \frac{a\,\sigma_{inf,1}}{\bar{E}_1}\, f\left(\frac{l}{a}, \frac{\bar{E}_2}{\bar{E}_1}\right), \tag{3}$$

where the dimensionless function f depends upon the aspect ratio of the H-shape crack l/a and the stiffness ratio $\bar{E}_2/\bar{E}_1$. Upon inserting eqn (3) into eqn (1), the energy drop per unit crack depth is

$$\Delta W = \frac{\sigma_{inf,1}^2}{\bar{E}_1} a^2 f\left(\frac{l}{a}, \frac{\bar{E}_2}{\bar{E}_1}\right). \tag{4}$$

This energy drop can be related to the energy release rate for H-shape tunneling crack G_{tun}, and to the energy release rate for plane-strain delamination G_d for each of the four delaminations of an H-shape crack, as follows.

Steady-state tunneling by an H-shape crack
The average energy release rate for unit advance of a tunneling H-shape crack, G_{tun}, is directly related to the energy drop ΔW by (Hutchinson and Suo [2], Beuth [5], Ho and Suo [7])

$$(2a + 4l)\, G_{tun} = \Delta W. \tag{5}$$

Also, the energy drop ΔW equals the energy required to form a mode I crack of length $2a$ in the central material 1 and four delaminations, each of length l. Upon designating the mode I toughness of material 1 as G_{Ic}, and the delamination toughness at the appropriate mode-mix as $G_{dc}(\psi(\hat{l}))$, the energy balance reads

$$\Delta W = (2a + 4l) G_{tun} = 2a\, G_{Ic} + 4l\, G_{dc}. \tag{6}$$

The remote stress for steady-state tunneling, $\sigma_{tun} = \sigma_{inf,1}$, follows from eqns (6) and (4) as

$$\sigma_{tun} = \sqrt{\frac{\bar{E}_1 (2a\, G_{Ic} + 4l\, G_{dc})}{a^2\, f(l/a,\, \bar{E}_2/\bar{E}_1)}}. \tag{7}$$

Plane-strain delamination
For the H-shape crack of Figure 2a the plane-strain energy release rate per unit advance of each delamination is

$$G_d = \frac{1}{4} \frac{\partial\, \Delta W}{\partial\, l}, \tag{8}$$

where the factor 4 reflects the number of delamination tips of the H-shape crack. Insertion of eqn (4) into eqn (8) yields

$$G_d = \frac{\sigma_{inf,1}^2}{4\bar{E}_1} a\, f'\left(\frac{l}{a}, \frac{\bar{E}_2}{\bar{E}_1}\right), \tag{9}$$

where f' represents the partial derivative $f' = \partial f/\partial l$. The remote stress for plane-strain delamination, $\sigma_d = \sigma_{inf,1}$ is obtained by combining eqn (9) with Griffith's criterion $G_d = G_{dc}$, and rearranging the expression to the form

$$\sigma_d = \sqrt{\frac{4\, \bar{E}_1\, G_{dc}}{a f'(l/a, \bar{E}_2/\bar{E}_1)}}. \tag{10}$$

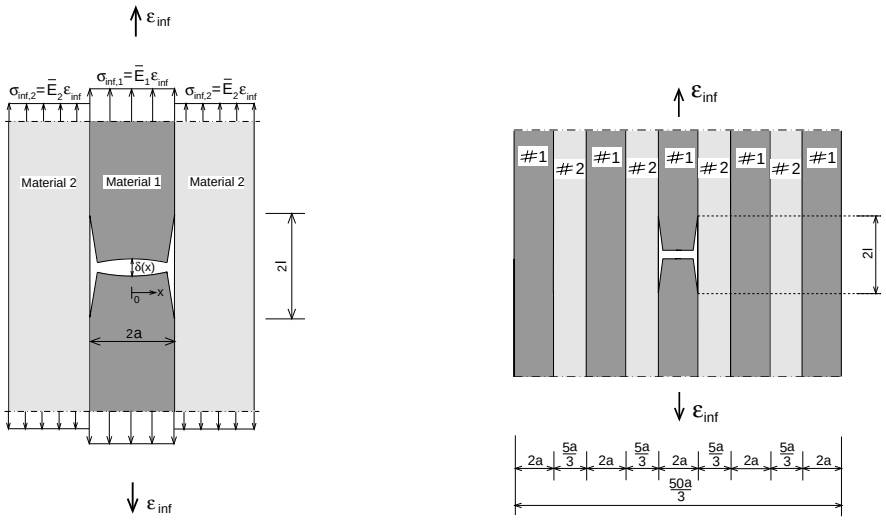

Figure 2: Plane-strain cracking: (a) H-shape crack as a results of a uniforom remote strain ε_{inf}. (b) H-shape crack in the centre layer of a laminate with a 5/4 lay-up.

3 CRACKING IN A 5/4 LAY-UP

Plane-strain delamination and steady-state tunneling is addressed for an H-shape crack in a 5/4 lay- up, as depicted in Figure 2b. Each layer of material 1 is of thickness 2a while the layers of material 2 have a thickness of 5a/3. This thickness ratio is typical of that used for the fibre-metal laminates GLARE and ARALL, where aluminium sheets of thickness 0.2 to 0.4 mm are bonded by somewhat thinner fibre/epoxy layers (Vlot and Gunnink [1]).

3.1 Modelling aspects

The configuration in Figure 2b has been modelled with the aid of the finite element program, ABAQUS Standard (Hibbitt, Karlsson & Sorensen, Inc., Pawtucket, RI, U.S.A.). The degree of symmetry is such that only one quadrant is meshed. Fixed and roller supports impose the required symmetry and prevent rigid body motion. The strip is taken to be sufficiently long for end effects to be negligible: the top and bottom faces of the 5/4 lay-up are at a distance $200a$ from the delamination tip. H-shape cracks with delamination lengths in the range $0.015 < l/a < 40$ have been considered, using 7 different element meshes. Mesh refinement studies have been performed to check the convergence of the solution. All finite element configurations comprise 16000 to 20000 plane-strain 8-node iso-parametric elements, with 3x3 Gauss quadrature. At the delamination tip, the square root singularity of the stress field is simulated by moving the mid-side nodes on the crack flanks to the 1/4 point nearest to the crack tip. Additionally, for each crack tip element, three neighbouring nodes are collapsed to the crack tip. A calculation of the critical stresses for steady-state tunneling, eqn (7), and for plane-strain delamination, eqn (10), of an H-shape crack requires the computation of: (i) the displacements of the nodes situated on the mode I crack faces, (ii) the path-independent J-integral at the delamination tip, (iii) the complex stress intensity factor at the delamination tip, $K = K_1 + iK_2$. More details on how these parameters are

obtained from the numerical analyses can be found in Suiker and Fleck [3].

3.2 Mode-mix

For the configuration in Figure 2b, the mode-mix ψ, which is evaluated at a specified distance 'a' ahead of the crack tip, has been computed as a function of the delamination length, l/a, and the results are presented in Figure 3 for selected values of stiffness mismatch, in the range 0.1 to 10.0. It is seen that the mode-mix at short crack lengths decreases from 72^o to 50^o with increasing stiffness ratio. For all stiffness ratios considered the mode-mix increases to 90^o with increasing l/a. Accordingly, the delamination tip closes and becomes a *pure mode II crack.*

Because the influence of mode I contact has been neglected in the analysis (i.e. crack face overlap is allowed to occur), the current analysis is, strictly speaking, not applicable when delamination is in pure mode II. However, Dollar and Steif [8] have demonstrated that for an H-shape crack in a homogeneous, infinite medium, the mode II stress intensity factor for a frictionless crack with and without crack face overlap only show minor differences. In other studies of mixed-mode delamination this feature was assumed to hold on the basis of heuristic reasoning. Thus, it is expected that the computed energy release rates are not greatly in error when the effect of crack surface contact is neglected.

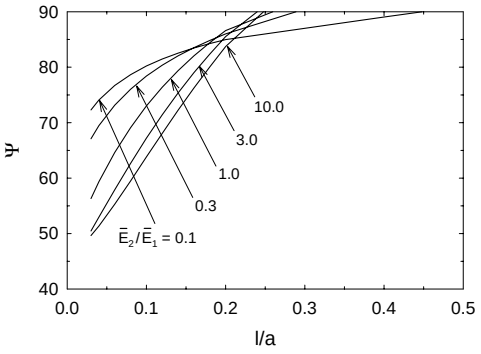

Figure 3: Mode-mixity ψ versus delamination length l/a.

3.2 Failure mechanism map

The *minimum* stress at which an H-shape crack will tunnel can be found from the numerical results by equating the remote stress for plane-strain delamination, eqn (10), with the tunneling stress, eqn (7), i.e. $\sigma_d = \sigma_{tun}$ (Suiker and Fleck [3]). A failure mechanism map can be constructed, in which the minimum tunneling stress $\sigma_{tun,min}$ is plotted against the toughness ratios G_{dc}/G_{Ic}, see Figure 4a. The figure can be used to estimate the (critical) tunneling stress for assumed values of G_{dc}/G_{Ic} and $\bar{E}_2/\bar{E}_1$. The three failure modes are displayed with the location of their boundaries indicated by dashed lines. Stable tunneling (*mechanism 2*) dominates the map for $\bar{E}_2/\bar{E}_1 < 1$. For each curve of tunneling stress versus toughness ratio the transition from one mechanism to another is indicated by a black dot. At low toughness ratios *mechanism 3* operates, whereas at higher toughness ratios and for $\bar{E}_2/\bar{E}_1 \geq 1$ *mechanism 1* operates; alternatively, at higher toughness ratios and for $\bar{E}_2/\bar{E}_1 < 1$ *mechanism 2* operates.

The corresponding values of the delamination length at tunneling are shown in Figure 4b as a function of the toughness ratio G_{dc}/G_{Ic}. For $\bar{E}_2/\bar{E}_1 = 3.0$ and 10.0 it is difficult to obtain the precise shape of the curve in the transition from *mechanism 1* ($(l/a)_{tun} = 0$) to *mechanism 3* ($(l/a)_{tun} \rightarrow \infty$); this transition occurs abruptly due to the small range of G_{dc}/G_{Ic} values over which *mechanism 2* is operational, see Figure 4a. Hence, for $\bar{E}_2/\bar{E}_1 = 3.0$ and 10.0 the anticipated trends for *mechanism 2* are represented by dashed lines. It is concluded from Figure 4b that H-shape cracking with a finite delamination

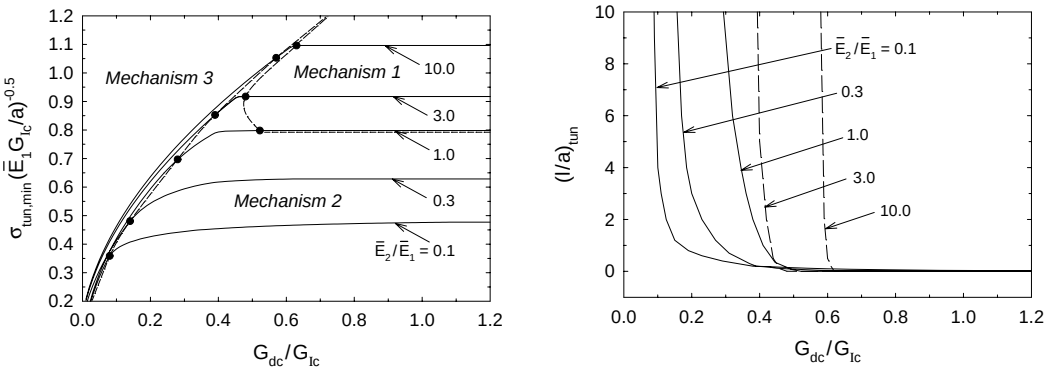

(a) (b)

Figure 4: Cracking in the centre layer of the 5/4 lay-up. (a) Minimum tunneling stress $\sigma_{tun,min}$ versus fracture toughness ratio G_{dc}/G_{Ic}. Dashed lines indicate the zones corresponding to the three failure mechanisms in Figure 1. (b) Delamination length $(l/a)_{tun}$ versus fracture toughness ratio G_{dc}/G_{Ic}.

length, exceeding $(l/a)_{tun} = 0.1$, only occurs over a narrow range of values for G_{dc}/G_{Ic}. For (relatively high) toughness ratios where $0 < (l/a)_{tun} < 0.1$, it becomes difficult experimentally to distinguish between *mechanism 2* with delamination present, and *mechanism 1* with delamination absent.

4 CONCLUDING REMARKS

Results for fracture patterns and geometries other than that in Figure 2b can be found in Suiker and Fleck [3]. Further, in Suiker and Fleck [3] the present model is used to predict experimental data for the residual strength of fibre-metal laminates. The application of the present model for the prediction of crack growth rates in fatigue experiments on laminates has been discussed recently in Suiker and Fleck [4].

REFERENCES

1. Vlot, A. and Gunnink, J.W. (eds.), *Fibre Metal Laminates - An Introduction.* Kluwer Academic Publishers, Dordrecht, 2001.
2. Hutchinson, J.W. and Suo, Z., Mixed mode cracking in layered materials. *Adv. Appl. Mech.* 29, 63–191, 1992.
3. Suiker, A.S.J. and Fleck, N.A., Crack tunneling and plane-strain delamination in layered solids. *Int. J. Frac.* 125, 1–32, 2004.
4. Suiker A.S.J. and Fleck, N.A., Modelling of steady-state fatigue crack growth in layered composites (Submitted). 2004.
5. Beuth, J.L., Cracking of thin bonded films in residual tension. *Int. J. Solids Struct.* 29, 1657–1675, 1992.
6. Cox, B.N. and Marshall, D.B., Crack initiation in fiber-reinforced brittle laminates, *J. Am. Ceram. Soc.* 79, 1181–1188, 1996.
7. Ho, S. and Suo, Z., Tunneling cracks in constrained layers. *J. Appl. Mech.* (ASME) 60, 890–894,1993.
8. Dollar, A. and Steif, P.S., The branched crack problem revisited. *J. Appl. Mech.* (ASME) 58, 584–586, 1991.